AGU ADVANCING EARTH AND SPACE SCIENCES

Earth's Future

RESEARCH ARTICLE
10.1029/2023EF003691

Economic Development Drives Massive Global Estuarine Loss in the Anthropocene

Nathalie W. Jung[1,2], Guan-hong Lee[1], Timothy M. Dellapenna[2,3], Yoonho Jung[1,3], Tae-Chang Jo[4], Jongwi Chang[1], and Steven M. Figueroa[1,5]

[1]Department of Oceanography, Inha University, Incheon, Republic of Korea, [2]Department of Marine and Coastal Environmental Sciences, Texas A&M University at Galveston, Galveston, TX, USA, [3]Department of Oceanography, Texas A&M University, College Station, TX, USA, [4]Department of Mathematics, Inha University, Incheon, Republic of Korea, [5]Department of Civil Engineering, Chungnam National University, Daejeon, Republic of Korea

Key Points:

- Globally, nearly ½ of today's estuaries have been directly altered by humans
- Land reclamation has resulted in the loss of ~250,000 acres (1,027 km^2) of estuarine surface area during the last 35 years
- Most human alterations and ecosystem loss happened in middle-income stages due to lacking conservation laws and policies

Supporting Information:

Supporting Information may be found in the online version of this article.

Correspondence to:

G. Lee,
ghlee@inha.ac.kr

Citation:

Jung, N. W., Lee, G., Dellapenna, T. M., Jung, Y., Jo, T.-C., Chang, J., & Figueroa, S. M. (2024). Economic development drives massive global estuarine loss in the Anthropocene. *Earth's Future*, *12*, e2023EF003691. https://doi.org/10.1029/2023EF003691

Received 3 MAY 2023
Accepted 24 JAN 2024

Author Contributions:

Conceptualization: Nathalie W. Jung, Guan-hong Lee, Timothy M. Dellapenna
Data curation: Nathalie W. Jung, Yoonho Jung, Jongwi Chang, Steven M. Figueroa
Formal analysis: Nathalie W. Jung, Yoonho Jung, Jongwi Chang, Steven M. Figueroa
Funding acquisition: Guan-hong Lee
Investigation: Nathalie W. Jung, Guan-hong Lee, Timothy M. Dellapenna, Tae-Chang Jo
Methodology: Nathalie W. Jung, Guan-hong Lee, Timothy M. Dellapenna, Tae-Chang Jo

Abstract

Estuaries have great ecological and economic value and sustain both population and economic growth. Global-scale analyses suggest that human activities drive estuarine area change but these projections neglect direct human-estuary interactions and socio-economic feedbacks. Here, we quantified area changes of 2,396 estuaries in response to recent human impacts (e.g., land reclamation, estuarine dam construction) and economic development between 1984 and 2019, and find that estuarine area shrank by 5,372 km^2 whereas upland submergence created 5,015 km^2 of estuarine area elsewhere. Approximately 44% ($n = 1,046$) of today's estuaries have been directly altered through land reclamation, estuarine dam construction, or a combination of both, and ~250,000 acres (1,027 km^2) of estuarine area have been directly converted to urban or agricultural fields. Nearly 90% (923 km^2) of land reclamation occurred in Asia linked to recent advances in economic development during the middle-income stage. Additional historical mapping and 5-year interval analyses revealed that while human alterations were insignificant during the low-income stages, estuaries were predominantly altered during their middle-income stages, where estuarine degradation is a common consequence of economic growth. However, this trend stabilizes in high-income countries with the adaption of conservation laws and policies. Together, our results indicate that large-scale estuarine loss can be avoided by preserving estuaries in low- and mid-income countries in the early stages of economic development.

Plain Language Summary

Estuaries are indentations along the coastline, where rivers meet the ocean. Estuaries are often called "nurseries of the sea" as not only animals but also humans commonly rely on them for nesting and breeding as well as tourism, fisheries, and recreational activities. The world's biggest cities are therefore often found in close proximity to an estuary. Historically, humans have actively altered estuaries through land reclamation or the construction of dams in an effort to create new land available for agriculture, infrastructure, housing, and/or industries so that estuaries have dramatically decreased in size throughout the last few decades and centuries. Interestingly, these changes mostly occurred during a country's middle-income stage, when conservation incentives were lacking, while human alterations were minimal during the low-income stage due to the lack of economic means. Concurrently with the country's economic success, estuaries tended to stabilize as increasing income allowed for more protective and renaturalization measures. Future preservation efforts should therefore focus on preserving estuaries in low- and middle-income countries in order to avoid ecosystem degradation.

1. Introduction

Modern-day estuaries (see Text S1 in Supporting Information S1 for a detailed definition) are among the most stressed and degraded natural systems in the world (Day et al., 2016), as increasing human impacts have significantly altered estuarine dynamics necessary to maintain an estuary's integrity (Nicholls et al., 2020; Nienhuis et al., 2020; Renaud et al., 2013; Tessler et al., 2015). Although estuaries and their ecosystem services are valued at approximately US$10,000 per hectare (Barbier et al., 2011; Kirwan & Megonigal, 2013), human development has modified estuaries worldwide through deforestation, urbanization, agricultural impoundment, and river flow diversion (Syvitski et al., 2005), where many estuarine tidal flats and wetlands have been converted to vast agricultural and urban areas (Syvitski & Saito, 2007). For example, large-scale land reclamation projects accounted for 60% of the observed estuarine surface area (ESA) loss in South Korea within the last 30 years (Jung et al., 2021). Although many laws and conservation efforts have been implemented to slow estuarine area loss and

Supervision: Guan-hong Lee
Validation: Jongwi Chang
Visualization: Nathalie W. Jung
Writing – original draft: Nathalie W. Jung
Writing – review & editing: Guan-hong Lee, Timothy M. Dellapenna, Steven M. Figueroa

the degradation of estuarine ecosystems, developing countries continue to convert estuarine systems to other land use types (Kirwan & Megonigal, 2013; Wang et al., 2014). Long-term estuarine sustainability, therefore, depends on the poorly understood interplay between natural and socio-economic factors so that it is no longer adequate to separate the effects of natural, economic, and social processes, which tend to maintain or disturb estuarine systems (Kirwan & Megonigal, 2013; Nicholls et al., 2020). A framework to evaluate human effects on estuarine development across the globe that specifically accounts for anthropogenic and economic processes is necessary to enhance the long-term resilience of these ecosystems. Here, we measured ESA changes for approximately 2,400 estuaries worldwide between 1984 and 2019 and compared them to direct human modifications and economic development to determine the timing and magnitude of anthropogenically driven global estuarine change over the last 35 years.

2. Materials and Methods

2.1. Identification of Estuaries and Estuarine Dams

To determine how estuaries responded to increasing human impacts during the last 35 years, we measured ESA change between 1984 and 2019 on a global scale and compared them to local human impacts, such as estuarine dam occurrence and land reclamation. To establish a global geodatabase of estuaries (i.e., estuaries and deltas [see Text S1 in Supporting Information S1 for a more detailed definition]), we manually identified an estuary as the transition point where channel width increased drastically from river to coastal embayment. Because previous remote sensing efforts found that river width data are generally most accurate and complete at width wider than 90 m (i.e., three Landsat pixels) (Allen & Pavelsky, 2018), we did not include estuaries with an estuary mouth width of less than 90 m. We extended this criterion to 3 km landward in order to ensure robust area change measurements. Additionally, we manually located the positions of estuarine dams in all identified estuaries. We note that our definition of estuarine dams includes dams located between the mouth and tidal limit of an estuary (i.e., the farthest upstream location where tidal fluctuations can be observed, see Section 2.2), which are generally constructed for freshwater storage and storm surge protection (Figueroa, Lee, Chang, et al., 2020; Figueroa, Lee, & Shin, 2020; Shin et al., 2019), as well as any structure that interferes with the upper estuarine flow (e.g., submerged weir). Conventional dams are located inland of the tidal limit and are typically constructed for freshwater retention, flood control, recreation, and hydroelectric power generation (Syvitski & Kettner, 2011). These inland dams result in enhanced deposition within the associated reservoir, reduced delivery of sediment downstream, and enhanced river incision and bank erosion downstream (Cashman et al., 2018; Hupp et al., 2009; James, 2019; Rodriguez et al., 2020). In contrast, estuarine dams reduce tidal currents due to loss of the tidal prism and thus the flushing capacity of the associated estuaries, resulting in highly elevated sedimentation and landward migration of sediment within these estuaries (Figueroa, Lee, Chang, et al., 2020; Figueroa, Lee, & Shin, 2020; Figueroa et al., 2022; Williams et al., 2013, 2014, 2015).

We extracted channel masks for estuaries worldwide using the global surface water data set, which provides the yearly extent of seasonal (tidal flats) and permanent (open water) water occurrence between 1984 and 2019 from high-resolution satellite images (Pekel et al., 2016). The identification of analyzable global estuaries therefore depends on the accuracy and availability of this data set. Validation processes at the pixel scale suggested that the global surface water data set is reliable for reconstructing global estuarine area changes (accuracy >95%) (Pekel et al., 2016). Because the global surface water data set identifies water occurrence based on the spectral properties of wavelengths measured by satellite sensors, "dry" or highly turbid rivers (i.e., rivers that cannot be distinguished from their surroundings based on color) cannot be captured by the data set and were therefore eliminated from further analyses. This approach is consistent with previous estimates of delta and river extents, where many estuarine systems along the northern African coast are generally excluded (Allen & Pavelsky, 2018; Nienhuis et al., 2020). We further excluded fjords and estuaries within polar and snow regions (i.e., Alaska, Canada, Russia, Finland, Sweden, and Norway) as they are commonly influenced by complicated glacio-marine sedimentary processes, such as meltwater streams and sea ice (Powell & Molnia, 1989). Our final data set includes estuaries on all major land masses except Antarctica, Greenland, and islands smaller than 10,000 km^2.

2.2. Estuarine Surface Area Change

To determine how estuaries have changed in size over the last 35 years, we measured the extent of global estuaries between 1984 and 2019 (Figure S1 in Supporting Information S1). Because running the algorithm for all estuaries worldwide would be computationally expensive, we clipped the global surface water data set to previously established country boundaries (http://www.marineregions.org/downloads.php) in order to analyze ESA change on a country-by-country basis. We then automatically delineated the estuarine extent in 1984 and 2019 by drawing a buffer around each manually located estuary point. We then erased the buffer area from the overall water occurrence in 1984 and 2019 to completely separate individual estuaries from the ocean. After deleting the ocean extent, we merged the previously deleted buffer area with the newly identified estuary extent. This approach includes further downstream portions of the estuary, and thus represents a broader perspective on anthropogenically driven change. We note that the temporal coverage of the first available channel mask may vary geographically depending on the availability of Landsat images and, therefore, the global surface water data set (Figure S2 in Supporting Information S1).

ESA and area change (i.e., ESA loss and gain, total and net change) were measured using the MATLAB MorphEst toolbox (Jung et al., 2021). MorphEst is a collection of analysis tools that use channel masks to automatically measure estuarine planform geometric features, such as estuarine length, ESA, and areal gain and loss due to natural or human factors (Jung et al., 2021). Comparisons with independent ESA and channel width measurements of 39 estuaries along the South Korean peninsula showed that MorphEst is a reliable tool for measuring estuarine spatial features (accuracy = 98%) (Jung et al., 2021).

To restrict area calculations to only the estuarine portion of the river channel mask, we measured estuarine length based on estuarine convergence (Savenije, 2005):

$$W = W_0\left(\exp\left(-\frac{x}{L}\right)\right),$$

where W is the width along the estuarine channel, W_0 is the width at the estuary mouth, x is the along-channel distance, and L is the estuarine length. We then compared our estuarine length estimates with observed depth-based length parameters from the UK (Prandle, 2004) and found that depth-based length estimates were generally longer than but comparable to width-based measurements (average difference ~4 km). In some cases, the measured estuarine length exceeded the upstream length of our channel mask data set. Here, the upstream estuarine extent was adjusted to the shorter data set in both time steps to ensure that measured changes in ESA were not an artifact of changes in length. Finally, the upstream extent of estuaries with an estuarine dam was restricted to the dam location.

MorphEst calculates the area of each estuary in 1984 and 2019, where area change is defined as the difference between the areal extent of both time steps. We note that total area change is defined as the summation of change regardless of positive or negative change, and net area change is defined as the summation of change with regard to positive and negative changes. Our methods explicitly calculate areas of gain and loss along the seaward margin of the 1984 and 2019 estuary extents and assume that negative changes in ESA are due to sediment accumulation or direct water-to-land conversion, whereas positive changes in ESA are due to erosion or submergence. Finally, we summarized changes in ESA across continents and national income classes (see Section 2.3) to identify geographic and economic patterns of area change (Figures S3–S7 in Supporting Information S1). We further differentiated between natural (i.e., estuaries with no estuarine dam, or loss due to land reclamation <10% (see Section 2.5)) and altered estuaries in order to determine the magnitude and economic impact of human alterations.

We tested whether our algorithm accurately calculated global ESA change by manually re-mapping areal change of 10 randomly selected estuaries in different portions of the world and across varying degrees of human impact. We manually located the historical and modern shorelines based on 1984 and 2019 Google Earth images and calculated area change between both time steps. On average, our algorithm correctly estimated 95%–99% of the manually digitized ESA changes. The remaining error was small and similar to the accuracy of the global surface water data set (>95%) on which this study is based (Pekel et al., 2016), so that differences between automated and manual area calculations may be caused by previous misinterpretations of water and land pixels.

2.3. Economic Dependency

We categorized countries by their income based on the gross national income per capita in current prices as defined by the World Bank (https://data.worldbank.org/indicator/NY.GNP.PCAP.CD) in an effort to understand how changing economic conditions may affect our perception of riveting feedbacks between society and estuarine morphology. The World Bank classifies countries into low-income, lower-middle-income, upper-middle-income, and high-income classes (Felipe et al., 2012). However, this income classification is unavailable before 1987 (Felipe et al., 2012). We therefore used Maddison's historical gross domestic product (GDP) per capita estimates (Maddison, 2010) and Felipe's GDP-based thresholds (Felipe et al., 2012) to reconstruct historical economic development for eight selected countries (see Section 2.4).

2.4. Historical Mapping

To determine how different stages of economic development affected estuarine morphology, the areal estuarine extent was calculated every 5 years between 1984 and 2019 using MorphEst (see Section 2.2) for eight representative countries (i.e., ∼10% of all analyzed countries and estuaries). Here, we chose countries at various income stages with substantial human modifications such as land reclamation and estuarine dams (Eertman et al., 2002; Jung et al., 2021; van Maren et al., 2016), as well as area change ranging from large changes during the mid-income stages to no change during the high-income stage. We then calculated the ESA extent at each time step and visually compared these extents to the timing of the majority of local dam constructions or land reclamation projects to identify the effect of human development on estuarine evolution (see Section 2.5). Because we manually removed portions of the estuary with low data quality (e.g., branches) to ensure that area changes were not an artifact of differences in quality, estimates of ESA may differ between the 5-year approach and the comparison between 1984 and 2019.

To measure changes in ESA of high-income countries during their middle-income stages, we additionally analyzed historical maps for three high-income countries. Because estuarine dam construction and land reclamation projects in many high-income nations mainly occurred prior to 1984, we specifically selected historical maps for countries with no areal change between 1984 and 2019, but which are well known to have highly modified estuaries (i.e., Germany, the Netherlands, and South Korea) (Eertman et al., 2002; Jung et al., 2021; van Maren et al., 2016). We established a database of approximately 150 historical maps between 1841 and 1974 (Table S1 in Supporting Information S1) and georeferenced each map to the 2016 ESRI World Imagery in ArcGIS by aligning at least five control points (e.g., road intersections) in all sets of historical maps with first order polynomials (Schieder et al., 2018). The average root mean square error associated with georeferencing of historical maps was 23–39 m, and the combined error in the x and y directions ($39 \text{ m} \times 39 \text{ m} = 0.0015 \text{ km}^2$) was less than measured changes in ESA (10–200 km^2). We then manually delineated the historical areal extent of estuaries along the land–sea boundary until the upstream extent which was previously defined by the estuarine length, dam location or the lowest quality channel mask.

Although previous work along the Chesapeake Bay and Gulf of Mexico coast of Florida, USA, suggests that historical maps are reliable for reconstructing the lateral position of the water–land boundary (Raabe & Stumpf, 2016; Schieder et al., 2018; Schieder & Kirwan, 2019), and German maps are considered accurate if constructed for military purposes (Scharfe, 2018; Wulf & Rujner, 2011), accuracy estimates for German, Dutch, and South Korean historical maps are limited. Here, we selected maps with the highest available resolution and spatial coverage (1:25,000 to 1:50,000). We then compared shoreline positions inferred from historical maps with soil surveys from the 1920s for South Korea and 1951 for Germany (Table S1 in Supporting Information S1) and found that the location of the water–land boundary on historical maps is consistent with that of historical soil survey maps from two sites in South Korea (i.e., Gomso Bay and Nakdong River) and two sites in Germany (i.e., Elbe and Weser). The shoreline location in South Korea based on 1974 historical maps is also similar to that of other maps sources (e.g., historical soil surveys) at the same location (Table S1 in Supporting Information S1), where slight differences in the shoreline position represent increasing land reclamation over time in response to a growing economy. Additionally, the positions of mainland features, such as sand bars, islands, and forests, were generally consistent with records from 1960s aerial images of a portion of the Han River near Seoul, South Korea (Table S1 in Supporting Information S1), and 1945 aerial images collected along the Elbe River in Germany and the Scheldt Estuary in the Netherlands (Table S1 in Supporting Information S1). Therefore, multiple lines of evidence in five disparate locations along the Korean and German coastlines all suggest that Korean, Dutch, and German historical maps are a reliable source for mapping century-scale shoreline change.

2.5. Direct Human Impacts

Global analyses showed that human impacts, such as river damming and deforestation, are a considerable driver of estuarine change (Nienhuis et al., 2020). We therefore compared our estimates of estuarine area change to human impacts, including estuarine dam occurrence (see Section 2.1) and land reclamation, to understand potential factors influencing change in estuarine area. We measured land reclamation using the 2020 global land cover data set GlobeLand30 (resolution: 30 × 30 m) (Chen et al., 2015). Here, MorphEst identified land use within areas of ESA loss for each estuary, where reclaimed land represents land that was classified as urban and/or agriculture by the global land cover map (Jung et al., 2021). We then calculated the proportion of land reclamation (i.e., agricultural and urban land) to natural land (i.e., forest, grassland, wetlands, and barren land). Misclassifications of ESA loss as water are likely due to the uncertainty of the land cover data set (80%; Chen et al., 2015). Here, we excluded the “unidentified” parts of ESA loss when calculating the proportion of loss due to land reclamation. We note that estuarine dams and land reclamation are not the only human activities within an estuary but rather are part of a wide spectrum of disturbances such as sand mining, dredging, deforestation, accelerated subsidence, etc. (e.g., Nienhuis et al., 2020; Koehnken et al., 2020; Wei, Cai, & Zhan, 2021; Wei, Cai, Zhan, & Li, 2021; Syvitski et al., 2022a, 2022b). Unfortunately, these human activities are not readily measurable from aerial imagery and are therefore not included in this study.

3. Results and Discussions

3.1. Assessment of Global Estuarine Distribution and Change

To determine global changes in ESA over the last 35 years, we determined the location and changes in the areal extent of global estuaries in 1984 and 2019 based on a previous global surface water change study (Pekel et al., 2016) (Figure 1 and Figures S1 and S2 in Supporting Information S1). We first manually identified the positions of estuaries worldwide with a river mouth width wider than 90 m ($n = 4{,}010$). Here, we found that estuaries occurred all over the world across a large continuum of environmental and topographic settings (Figure 1a, Table S2). Interestingly, nearly half of the identified estuaries ($n = 1{,}879$; 47%) were located within Asia (including Russia). The remainder were somewhat evenly distributed across the globe, with the majority of estuaries located in North America ($n = 512$; 13%), Africa ($n = 435$; 11%), Oceania ($n = 374$; 9%), and Europe ($n = 362$; 9%), and the least number of estuaries occurring in South America ($n = 232$; 6%) and Central America ($n = 216$; 5%) (Figure 1a, Table S2).

Next, we measured area change of global estuaries over the study period based on a recent global water change analysis (Pekel et al., 2016). Here, we removed estuaries with low data quality ($n_1 = 608$) as well as fjords and estuaries within polar and snow regions ($n_2 = 1{,}006$; $n_{1+2} = 1{,}614$) (see *Methods*, Table S2). The remaining 2,396 estuaries occupied 92,917.6 ± 293.4 (1 SD) km^2 of surface area in 1984 and 92,560.8 ± 287.6 km^2 in 2019 (Figure 1b, Table S2). During this period, estuaries shrank in area by 5,372 ± 171 km^2 (5.8%), while 5,015 ± 119 km^2 (5.4%) of new estuarine area was created elsewhere, resulting in a total area change of 10,387 ± 147 km^2. Although area change varied substantially on estuarine, national, and continental scales, summed across the entire world, estuaries experienced a mere net loss of 357 ± 97 km^2 or 0.4%.

We then investigated spatial patterns of ESA change across continents and countries between 1984 and 2019 (Figure 1b, Figures S3–S7 in Supporting Information S1, Table S2 and Table S3 in Supporting Information S1). Gross area gain mostly occurred in Asia, with an increase of 2,349 ± 21 km^2 (47%). In contrast, NA experienced only a small increase in ESA of 223 ± 4 km^2 (5%). Africa and Oceania experienced similar increases in estuarine area of 565 ± 8 km^2 (11%) and 451 ± 5 km^2 (9%), respectively. European ESA increased by 369 ± 4 km^2—a 7% increase for the continent. Estuaries in Central America increased by 70 ± 1 km^2 (1%), and South American estuaries increased by 988 ± 34 km^2 (20%). Overall, approximately 62% of the estuaries worldwide experienced a net area gain, though only 18% of all estuaries exceeded a net area gain of 10% (Figure 1b). The majority of ESA gain can generally be attributed to a combination of reduced sediment supply due to drainage basin dams (Nienhuis et al., 2020), estuarine erosion (Latrubesse et al., 2017), enhanced subsidence (Al Mukaimi et al., 2018; Dellapenna et al., 2022), and eustatic sea-level rise (Kennish, 2002). However, our analyzes may be insufficient to identify the exact cause for estuarine expansion because the combined effects of natural and human processes are too complex to measure with simple remote sensing techniques, and more process-based analyses are necessary to discern the role of climate change, human modifications, and sediment dynamics in estuarine expansion.

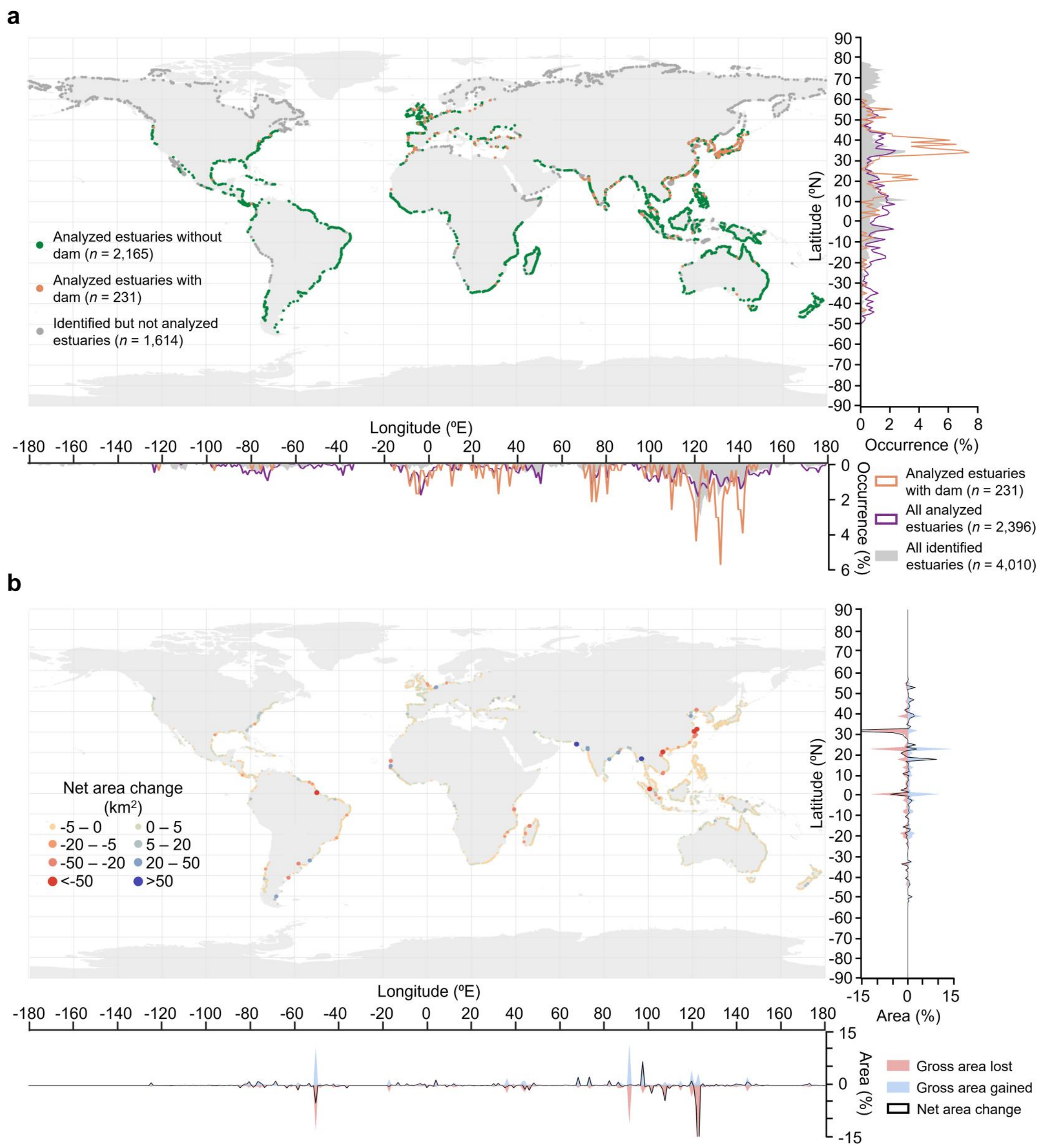

Figure 1. *Global estuarine areal change*. (a) Global occurrence of estuaries and dams. The location of estuaries and dams was manually identified. Green dots indicate analyzed estuaries without dam ($n = 2{,}165$), orange dots indicate analyzed estuaries with dam ($n = 231$), and gray dots indicate only identified, but not analyzed estuaries ($n = 1{,}614$). Line plots show the sum of all analyzed estuaries (purple line), all analyzed estuaries with an estuarine dam (orange line) and all identified (analyzed and not analyzed) estuaries (black shaded area) per 1° latitude and longitude relative to the total number of all analyzed estuaries ($n = 2{,}396$), all analyzed estuaries with an estuarine dam ($n = 230$) and all identified estuaries ($n = 4{,}010$) worldwide, respectively. Approximately 10% of all analyzed estuaries worldwide are dammed, with hotspots in Asia and Europe. (b) Net change in estuarine surface area (ESA) (km^2) per estuary. Line plots show gross area gained and lost as well as net estuarine area change per 1° latitude and longitude relative to the total area of gross gain and loss and net area change worldwide, respectively. Hotspots of ESA loss occur in Asia.

Spatial comparisons revealed that ESA loss is more geographically concentrated than gain (Figure 1b). Fifty-five percent of the ESA loss (2,934 ± 29 km^2) occurred in Asia, much of which (84%) was concentrated in only five countries (i.e., China, Bangladesh, Vietnam, Indonesia, and India) (Figure 1b, Table S2). China has the greatest ESA loss with more than 1,250 km^2 of ESA lost between 1984 and 2019 (Figure 1b). In contrast, estuaries in North and Central America lost an area of less than 100 km^2 (4%), those in Europe and Oceania lost 239 ± 3 km^2 (4%) and 292 ± 4 km^2 (5%), respectively, and African estuaries lost 605 ± 9 km^2 (a decrease of ~11% for the continent). South America accounts for 21% of the global area loss (1,145 ± 44 km^2). Although natural processes

10.1029/2023EF003691

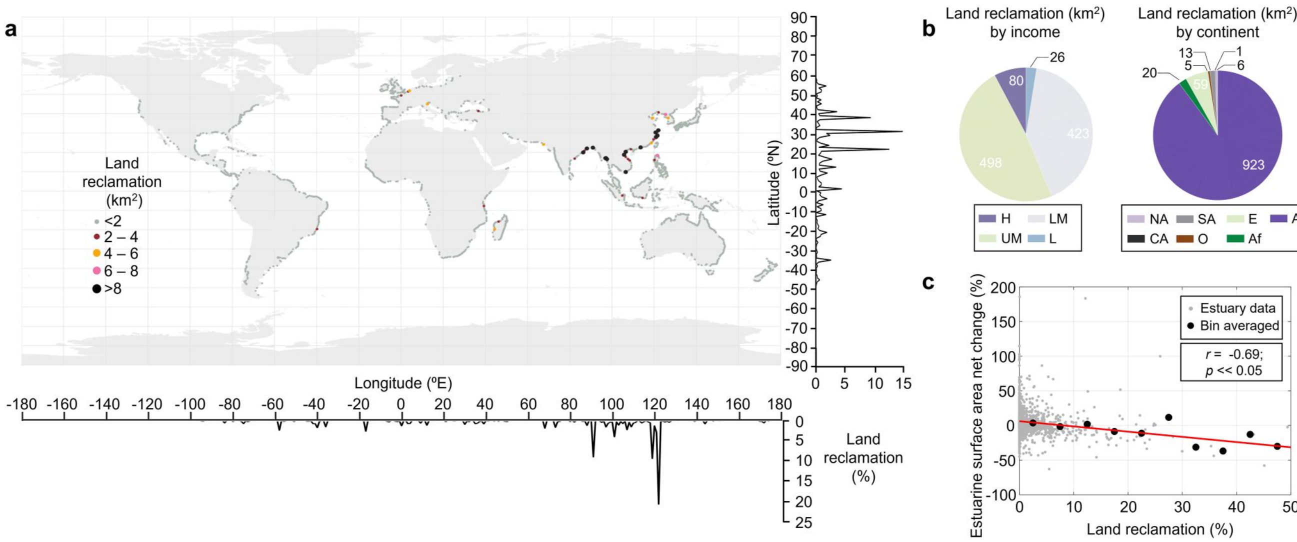

Figure 2. Effects of land reclamation on estuarine surface area (ESA) change. (a) Global extent of land reclamation. The map shows ESA loss due to land reclamation between 1984 and 2019 (km^2). Line plots show loss due to land reclamation per 1° latitude and longitude relative to total loss due to land reclamation worldwide (1,027 km^2). Approximately ¼ of global area loss was due to land reclamation, with hotspots in Asia. (b) Loss due to land reclamation summarized by income (left) and continent (right), where L, low income; LM, lower middle income; UM, upper middle income; H, high income; NA, North America; CA, Central America; SA, South America; O, Oceania; E, Europe; Af, Africa; As, Asia. The majority of land reclamation occurred in middle-income countries as well as in Asia. (c) Effects of land reclamation on ESA change. Bin averaged net ESA and land reclamation were significantly correlated ($r = -0.69$, $p \ll 0.05$), indicating that estuaries generally contracted in regions with large human modifications.

such as sediment accumulation may facilitate ESA loss in pristine environments with large estuarine systems (e.g., South America), much of the overall ESA loss can be linked to hotspots of human alterations, including the construction of estuarine dams (as defined in *Methods*, Figure 1a) and large-scale land reclamation projects (Figure 2a).

3.2. Direct Human-Estuary Interaction

Global analyses identified rapid ESA loss and found that human interferences have become a considerable driver of these morphologic changes (Nienhuis et al., 2020). Here, we manually identified the locations of 231 estuarine dams in all identified estuaries (Figure 1a, Table S2). We then measured the extent of local land reclamation to understand the magnitude of anthropogenically driven estuarine degradation. We identified land use within areas of ESA loss for each estuary, where reclaimed land was defined as land classified as urban and/or agricultural by a global land cover map (Chen et al., 2015; Jung et al., 2021). Our results suggest that humans have considerably modified estuaries worldwide (Figures 1a and 2), as 44% ($n = 1,046$) of all analyzed estuaries worldwide have been directly modified by humans whether through land reclamation ($n = 995$; 42%) (i.e., number of estuaries with a loss due to land reclamation >10%), the construction of estuarine dams ($n = 231$; 10%), or both ($n = 180$, 8%). Here, more than 90% of estuarine dams are located in Asia ($n = 165$) and Europe ($n = 45$) (Figure 1a), and almost 90% of the global ESA loss due to land reclamation occurred in Asia alone (923 ± 11 km^2) (Figure 2b), spatially coinciding with hotspots of ESA loss (Figure 1b). Summed across the entire world, land reclamation accounted for 25% of the total ESA loss between 1984 and 2019 (1,027 ± 7 km^2).

As large-scale coastal reclamation efforts and estuarine dam construction tend to occur nearly simultaneously (Figueroa, Lee, Chang, et al., 2020; Figueroa, Lee, & Shin, 2020; Williams et al., 2013, 2014), it is not surprising that estuaries with an estuarine dam were generally associated with a higher degree of land reclamation compared with those without an estuarine dam. For example, the average ESA loss due to land reclamation in estuaries with an estuarine dam was ∼40%, while the average ESA loss due to land reclamation in estuaries without an estuarine dam was less than 20%. Simple linear regressions suggest ESA change was significantly correlated with land reclamation ($r = -0.69$; $p < 0.05$) (Figure 2c), indicating that ESA loss tends to be higher in regions with high human development and that direct human alterations have become a crucial component in determining estuarine geomorphic processes. However, previous work showed that the magnitude of land reclamation largely depends

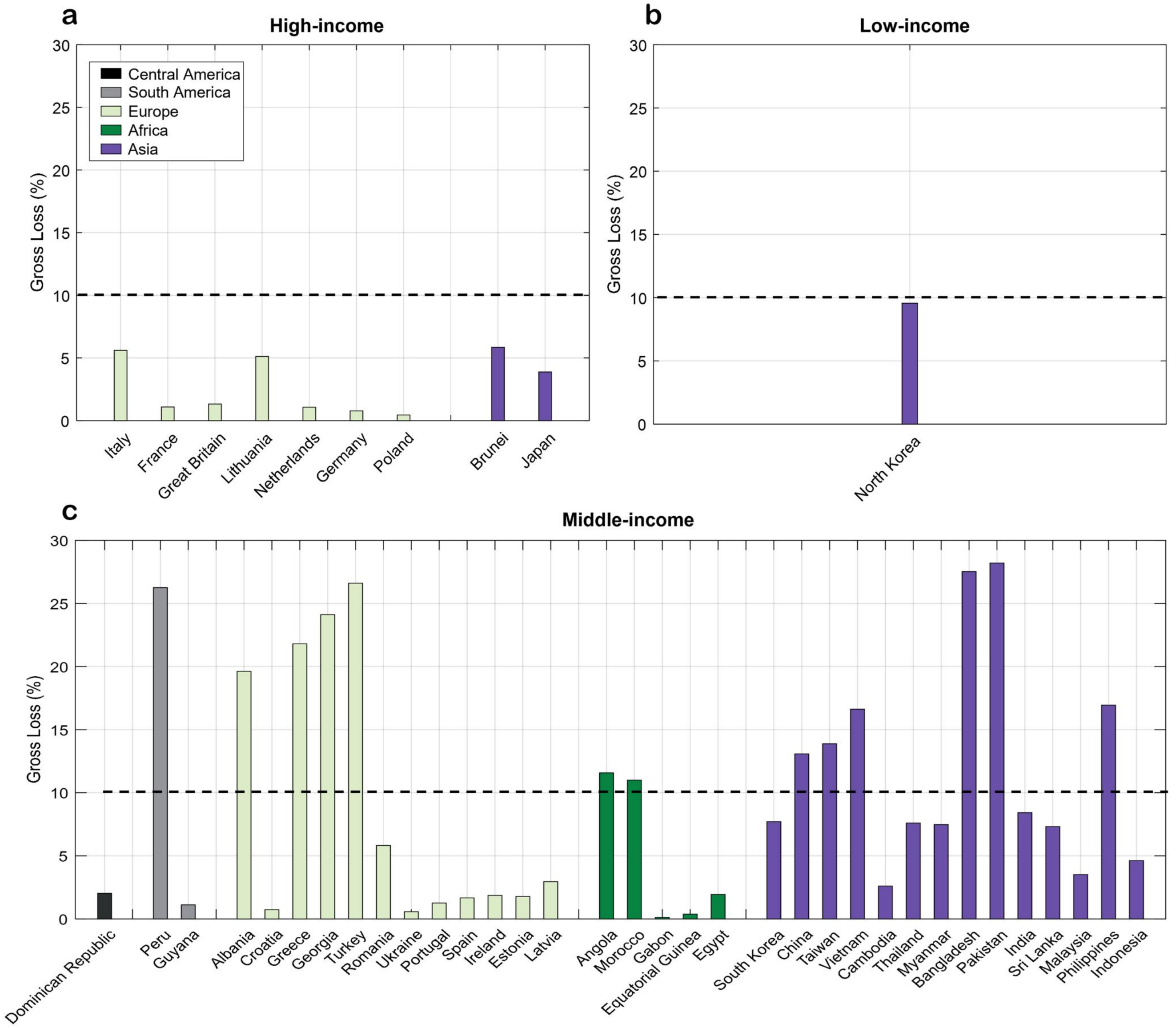

Figure 3. Economic dependence of estuarine surface area (ESA) change. Gross area loss (%) relative to ESA at time 1 for each analyzed high- (a), low- (b), and middle-income (c) country with slight human modifications (i.e., loss due to land reclamation >10%). The black dashed lines represent a gross loss of 10%. High-income countries only include countries that remained in the high-income stage during the study period (i.e., 1984–2019). Gross loss was below 10% in high- and low-income countries, whereas ESA loss in the majority of middle-income countries exceeded 10% due to large-scale land reclamation projects and recent estuarine dam constructions. Overall, the magnitude and timing of ESA change largely depend on the economic development and local policies of individual countries.

on the economic development, where the intentional conversion of estuarine environments to urban complexes is expected to slow down as countries achieve higher economic standards (Kirwan & Megonigal, 2013), but this idea remains largely untested.

3.3. Economic Dependency

We categorized and examined ESA loss based on income classes over the last 35 years to understand the role of socio-economic feedbacks in determining estuarine change (Figure 3 and Figure S8 and Table S4 in Supporting Information S1). Our results show that significant ESA loss occurred only during the middle-income stages (as defined in Section 2.3), with almost 50% of the analyzed middle-income countries exceeding a gross loss of 10% (Figure 3), perhaps due to large-scale land reclamation projects and recent estuarine dam constructions. On the other hand, no significant loss occurred for low- and high-income countries. Similarly, our results show that

10.1029/2023EF003691

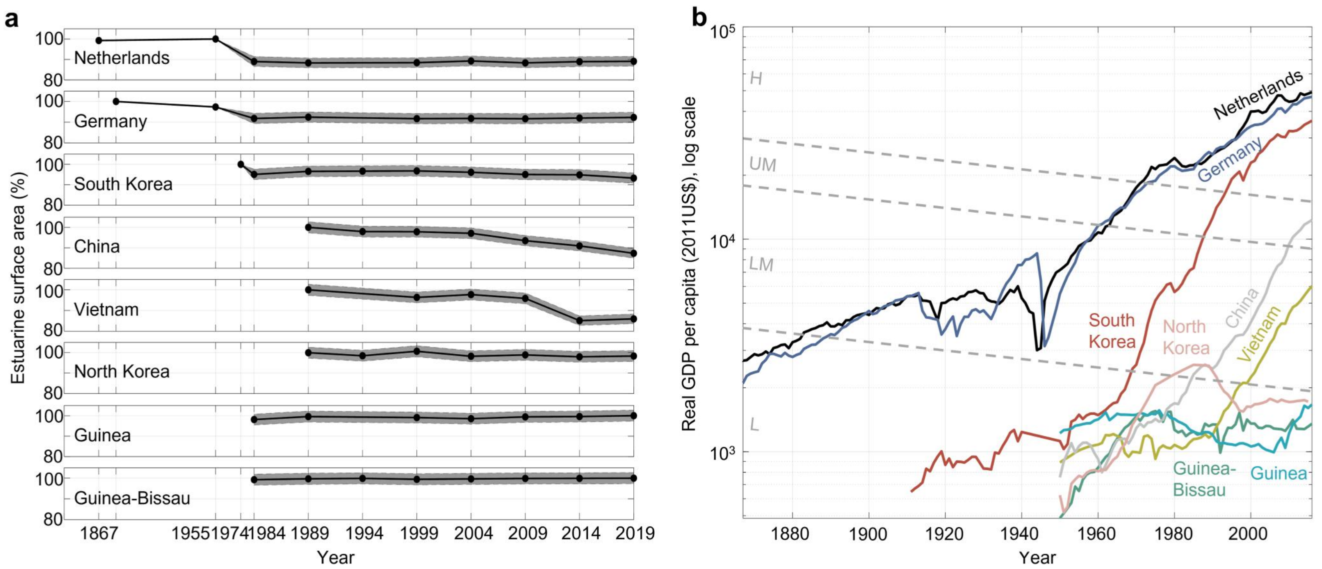

Figure 4. Estuarine surface area (ESA) change versus economic growth through time. (a) Estuarine area change of eight representative countries over time. ESA (%) was measured relative to the maximum ESA for each country. Five-year intervals between 1984 and 2019 were based on the global surface water data set (Pekel et al., 2016), while the pre-1984 areas for the Netherlands, Germany, and South Korea were based on historical maps. Areas of error are based on the minimum accuracy of water detection based on Pekel et al. (2016) for periods between 1984 and 2019 and the root mean square error of historical maps for periods before 1984. Countries are sorted from high-income countries at the top to low-income countries at the bottom. (b) Gross domestic product (GDP) per capita of all eight representative countries over time. Thresholds for each income class were estimated from Felipe et al. (2012), where L, low income; LM, lower middle income; UM, upper middle income; H, high income. ESA loss generally occurred after estuarine dam constructions and land reclamation efforts (e.g., South Korea, Germany, the Netherlands, China, and Vietnam) during the middle-income stage. Estuaries with no surface area change were mainly located in low-income (i.e., relatively "natural" state) or high-income countries, where active coastal management policies result in the preservation of coastal systems.

nearly 90% of global land reclamation occurred in countries with middle-income status in 2019 (921 km^2), with significantly less land reclamation occurring in countries currently with high-income status (80 km^2 or 8%) (Figure 2b). This suggests that the overall magnitude and timing of human-induced ESA change largely depend on the economic development and local policy decisions regarding the value of estuarine systems.

Figure 3 presents ESA change between 1984 and 2019, however, not all income periods were considered for all countries, especially high-income countries. To further test our hypothesis of economic dependency, we reconstructed short-term (i.e., 5-year intervals between 1984 and 2019) and long-term (>100 years for three additional countries) ESA change for selected countries and compared this change to their economic development (Table S5 in Supporting Information S1). Here, we chose countries at various income stages and continents that are well-known to have been heavily modified through land reclamation and the construction of estuarine dams in the past (i.e., loss due to land reclamation >10%: North Korea, Vietnam, China, South Korea, Germany, and the Netherlands) (Figure 3) (e.g., Eertman et al., 2002; Jung et al., 2021; van Maren et al., 2016). Because estuaries in low-income countries are generally expected to be free from human alterations due to the lack of economic means (i.e., loss due to land reclamation <10%), we further included temporal analyses of areal change for estuaries in Guinea and Guinea-Bissau in an effort to include estuaries from different continents with acceptable resolution.

ESA in low-income countries remained nearly stable between 1984 and 2019, as the majority of estuaries are still in their "natural" state (Figure 4, Figure S9 in Supporting Information S1). ESA in high-income countries was also unchanged during this period likely due to the adoption of conservation laws and policies (Arrow et al., 1995; Smits et al., 2006; Tessler et al., 2015). In contrast, more than 75% of ESA change between 1984 and 2019 occurred in middle-income countries (Figure S3 in Supporting Information S1), where increased environmental degradation has become an inevitable consequence of economic development (Arrow et al., 1995). Interestingly, similar geomorphic changes were visible in high-income countries during their middle-income stages. In highly altered, high-income countries, such as Germany, the Netherlands, and South Korea, major ESA loss mainly occurred during their middle-income stages following estuarine dam construction and land reclamation projects (Figure S9 in Supporting Information S1).

This research focused on ESA change over the last 35 years and therefore excludes historical land reclamation in current high-income countries, so that our assessment likely underestimates the major contribution humans make to estuarine degradation. Although South Korea, Germany, and the Netherlands account for only 3% of the total number of analyzed estuaries in high-income countries, local land reclamation and estuarine dam constructions resulted in the loss of 382 km^2 of ESA prior to 1984 (i.e., 37% of the total loss due to land reclamation measured between 1984 and 2019) (Figure 4). These observations suggest that when integrated over larger temporal and spatial scales, direct human impacts have potentially led to massive and widespread loss of crucial estuarine habitats since the beginning of coastal development.

4. Conclusions and Broader Implications

Our observations suggest that human alterations driven by economic development largely control the position of estuarine shorelines, where nearly half of today's estuaries have been modified by humans worldwide at some point in the past and large-scale land reclamation projects have resulted in the loss of nearly 250,000 acres (1,027 km^2 or 19% of the global ESA loss) of ESA during the last 35 years alone. While the processes that cause estuarine change are ultimately quite complex, deviations between land reclamation and ESA change confirm that the local economic development and therefore the importance of conservation incentives influence the pace of estuarine habitat change in highly developed countries. The lack of economic means in low-income countries has minimized (anthropogenically driven) estuarine change, whereas increasing wealth and the lack of conservation efforts in middle-income countries has lead to massive global estuarine loss (Figure S9 in Supporting Information S1). However, this trend stabilizes in high-income countries with the adaption of conservation laws and policies. For example, many high-income countries are now attempting to restore their degraded estuaries through dam removal in an effort to restore vital ecosystem functions and economic benefits (e.g., the United States (Crane, 2009), Japan (Young & Ishiga, 2014), the Netherlands (Ysebaert et al., 2016), etc.). Together, decisions to protect or modify estuarine habitats therefore largely depend on the local economy and represent a crucial determinant of estuarine morphologic change.

For more than 30 years, estuarine vulnerability research has mainly focused on the impacts of river damming, deforestation, and sea-level rise on estuarine geomorphic change (Nienhuis et al., 2020; Syvitski et al., 2005, 2009; Syvitski & Kettner, 2011; Syvitski & Saito, 2007). However, direct human alterations, such as estuarine dams and land reclamation, have only recently been recognized as major threats to estuarine sustainability (Chang et al., 2020; Figueroa, Lee, & Shin, 2020; Jung et al., 2021; Sengupta et al., 2023; Williams et al., 2013). Studies across the world have shown that the construction of estuarine dams greatly alters sediment transport dynamics within the estuary by reducing the tidal prism, thereby drastically increasing sediment deposition within the estuary (Barusseau et al., 1998; Figueroa, Lee, & Shin, 2020; Kim et al., 2006; Traini et al., 2015; Williams et al., 2013; Wolanski et al., 2001). In some cases, this may even lead to the reorganization of the entire estuary, causing a shift from a relatively tide-dominated system toward an increasingly wave-dominated system with barrier islands (Williams et al., 2013) or coming close to a coastal embayment–type functioning (Figueroa et al., 2022; Traini et al., 2015). Further constraints on sediment transport dynamics may arise from channel dredging, sand mining, and upstream river damming, which have previously been observed to cause major disturbances to estuarine systems such as channel incision, sediment redistribution, and downstream sediment load reduction (Koehnken et al., 2020; Wei, Cai, & Zhan, 2021; Wei, Cai, Zhan, & Li, 2021; Syvitski et al., 2022a). For example, a combination of channel deepening, sediment excavation, and river impoundment along the Pearl River Estuary, China, effectively reduced 30% of the total sediment load between 1980 and 2015 and therefore drastically accelerated the rate and areal extent of local erosion (Wei, Cai, & Zhan, 2021). Nevertheless, changes in water area and shoreline position due to erosion were several orders of magnitudes less (0.07 m $year^{-1}$) than human driven changes following large-scale land reclamation projects (64.8–256.3 m $year^{-1}$) (Wei, Cai, & Zhan, 2021), where estuaries are being progressively filled in resulting in the loss of valuable tidal flats (Cheng et al., 2020; van der Wal et al., 2002). This loss of estuarine ecosystems contributes substantially to biological invasions, declining water quality, destruction of important nursery and feeding grounds, and decreased storm surge protection (Barbier et al., 2011; Wang et al., 2014). For example, the reclamation of almost 1,000 km^2 of tidal flats in the Qiantang estuary, China, caused severe flooding in nearby cities and resulted in the loss of benefits from China's estuarine ecosystem of about US$4,600 million per year over the past 50 years (Wang et al., 2014). Land reclamation can therefore no longer be considered “costless” by coastal managers (Barbier et al., 2011), as the asset value of protecting existing estuarine habitats (US$6,996 per hectare) far outweighs the asset value of restored habitats (US$5,630 per hectare) (Johnston et al., 2002). Given the rate and scale at which estuarine habitats are being converted to land worldwide (Figures 2 and 4), more attention must be paid to preserving the benefits of existing estuarine habitats—particularly those in early-stage mid-income countries—in order to prevent substantial estuarine degradation and the loss of further important ecosystem service values.

Data Availability Statement

The global surface water data set can be downloaded from Google Earth Engine or https://global-surface-water.appspot.com/download and a more detailed description of the data set can be found in Pekel et al. (2016). Previously established country boundaries can be found at http://www.marineregions.org/downloads.php. The MATLAB toolbox MorphEst can be downloaded from https://www.mathworks.com/matlabcentral/fileexchange/86173-morphest-estuary-planform-geometry. Information on the gross national income per capita can be obtained by the World Bank (https://data.worldbank.org/indicator/NY.GNP.PCAP.CD), and information on the GDP per capita can be found in Maddison (2010). Historical maps of South Korea can be obtained from http://map.ngii.go.kr and https://www.koreanwar.org/html/korean-war-topo-maps.html. We note that historical maps of South Korea from http://map.ngii.go.kr are only accessible in South Korea. Historical maps from Germany can be found at https://www.landkartenarchiv.de/deutschland_messtischblaetter_1.php. Historical aerial images from Germany and the Netherlands can be downloaded from https://ncap.org.uk/search?keywords=Germany#free-text=yes&zoom=3&lat=6675890.31434&lon=1153060.03172&layers=BT and https://ncap.org.uk/search?keywords=Netherlands#free-text=yes&zoom=3&lat=7038498.30241&lon=147672.20635&layers=BT, respectively. Historical maps from the Netherlands can be found at https://www.uu.nl/en/special-collections/search-the-collection/the-best-access/georeferencing#Recently%20georeferenced%20maps and https://hub.arcgis.com/maps/esrinl-content::historische-topografische-data-1950/about. Finally, soil survey maps from South Korea and Germany can be downloaded from http://nationalatlas.ngii.go.kr/pages/page_2291.php and https://esdac.jrc.ec.europa.eu/resource-type/national-soil-maps-eudasm?type=All&field_data_continent_tid_selective=1266&field_data_country_country_selective=DE&field_data_cont_coverage_value=0&page=1, respectively. The land cover maps can be downloaded from https://shop.geospatial.com/publication/XV1CCGGP7TGJ44PGKT0RJ15V47/GlobeLand30-30-meter-Global-Land-Cover, and a more detailed description of the data set can be found in Chen et al. (2015).

Acknowledgments
This research was supported by Basic Science Research Program (2017R1D1A1B05033162) and Center for Anthropocene Studies (2018R1A5A7025409) through the National Research Foundation of Korea (NRF). We would like to thank Bogang Jun for her assistance with GDP calculations.

References

Allen, G. H., & Pavelsky, T. M. (2018). Global extent of rivers and streams. *Science*, *361*(6402), 585–588. https://doi.org/10.1126/science.aat0636

Al Mukaimi, M. E., Dellapenna, T. M., & Williams, J. R. (2018). Enhanced land subsidence in Galveston Bay, Texas: Interaction between sediment accumulation rates and relative sea level rise. *Estuarine, Coastal and Shelf Science*, *207*, 183–193. https://doi.org/10.1016/j.ecss.2018.03.023

Arrow, K., Bolin, B., Costanza, R., Dasgupta, P., Folke, C., Holling, C. S., et al. (1995). Economic growth, carrying capacity, and the environment. *Ecological Economics*, *15*(2), 91–95. https://doi.org/10.1016/0921-8009(95)00059-3

Barbier, E. B., Hacker, S. D., Kennedy, C., Koch, E. W., Stier, A. C., & Silliman, B. R. (2011). The value of estuarine and coastal ecosystem services. *Ecological Monographs*, *81*(2), 169–193. https://doi.org/10.1890/10-1510.1

Barusseau, J. P., Bǎ, M., Descamps, C., Diop, E. S., Diouf, B., Kane, A., et al. (1998). Morphological and sedimentological changes in the Senegal River estuary after the construction of the Diama dam. *Journal of African Earth Sciences*, *26*(2), 317–326. https://doi.org/10.1016/s0899-5362(98)00014-1

Cashman, M. J., Gellis, A., Sanisaca, L. G., Noe, G. B., Cogliandro, B., & Baker, A. (2018). Bank-derived material dominates fluvial sediment in a suburban Chesapeake Bay watershed. *River Research and Applications*, *34*(8), 1032–1044. https://doi.org/10.1002/rra.3325

Chang, J., Lee, G., Harris, C. K., Song, Y., Figueroa, S. M., Schieder, N. W., & Lagamayo, K. D. (2020). Sediment transport mechanisms in altered depositional environments of the Anthropocene Nakdong Estuary: A numerical modeling study. *Marine Geology*, *430*, 106364. https://doi.org/10.1016/j.margeo.2020.106364

Chen, J., Chen, J., Liao, A., Cao, L., Chen, X., He, C., et al. (2015). Global land cover mapping at 30m resolution: A POK-based operational approach [Dataset]. ISPRS Journal of Photogrammetry and Remote Sensing, *103*, 7–27. https://doi.org/10.1016/j.isprsjprs.2014.09.002

Cheng, Z., Jalon-Rójas, I., Wang, X. H., & Liu, Y. (2020). Impacts of land reclamation on sediment transport and sedimentary environment in a macro-tidal estuary. *Estuarine, Coastal and Shelf Sciience*, *242*, 106861. https://doi.org/10.1016/j.ecss.2020.106861

Crane, J. (2009). "Setting the river free": The removal of the Edwards dam and the restoration of the Kennebec River. *Water History*, *1*(2), 131–148. https://doi.org/10.1007/s12685-009-0007-2

Day, J. W., Agboola, J., Chen, Z., D'Elia, C., Forbes, D. L., Giosan, L., et al. (2016). Approaches to defining deltaic sustainability in the 21st century. *Estuarine, Coastal and Shelf Science*, *183*, 275–291. https://doi.org/10.1016/j.ecss.2016.06.018

Dellapenna, T. M., Hoelscher, C., Hill, L., Critides, L., Salgado (Bartlett), V., Bell, M., et al. (2022). Hurricane Harvey delivered a massive load of Mercury-rich sediment to Galveston Bay, TX, USA. *Estuaries and Coasts*, *45*(2), 428–444. https://doi.org/10.1007/s12237-021-00990-7

Eertman, R. H. M., Kornman, B. A., Stikvoort, E., & Verbeek, H. (2002). Restoration of the Sieperda Tidal Marsh in the Scheldt Estuary, the Netherlands. *Restoration Ecology*, *10*(3), 438–449. https://doi.org/10.1046/j.1526-100x.2002.01034.x

Felipe, J., Abdon, A., & Kumar, U. (2012). Tracking the middle-income trap: What is it, Who is in it, and Why? https://doi.org/10.2139/ssrn.2049330

Figueroa, S. M., Lee, G., Chang, J., & Jung, N. W. (2022). Impact of estuarine dams on the estuarine parameter space and sediment flux decomposition: Idealized numerical modeling study. *Journal of Geophysical Research: Oceans*, *127*(5), e2021JC017829. https://doi.org/10.1029/2021jc017829

Figueroa, S. M., Lee, G., & Shin, H.-J. (2020). Effects of an estuarine dam on sediment flux mechanisms in a shallow, macrotidal estuary. *Estuarine, Coastal and Shelf Science*, *238*, 106718. https://doi.org/10.1016/j.ecss.2020.106718

Figueroa, S. M., Lee, G., Chang, J., Schieder, N. W., Kim, K., & Kim, S. Y. (2020). Evaluation of along-channel sediment flux gradients in an Anthropocene estuary with an estuarine dam. *Marine Geology*, *429*, 106318. https://doi.org/10.1016/j.margeo.2020.106318

Hupp, C. R., Pierce, A. R., & Noe, G. B. (2009). Floodplain geomorphic processes and environmental impacts of human alteration along Coastal Plain Rivers, USA. *Wetlands*, *29*(2), 413–429. https://doi.org/10.1672/08-169.1

James, L. A. (2019). Impacts of pre- vs. postcolonial land use on floodplain sedimentation in temperate North America. *Geomorphology*, *331*, 59–77. https://doi.org/10.1016/j.geomorph.2018.09.025

Johnston, R. J., Grigalunas, T. A., Opaluch, J. J., Mazzotta, M., & Diamantedes, J. (2002). Valuing estuarine resource services using economic and ecological models: The Peconic estuary system study. *Coastal Management*, *30*(1), 47–65. https://doi.org/10.1080/08920750252692616

Jung, N. W., Lee, G., Jung, Y., Figueroa, S. M., Lagamayo, K., Jo, T. C., & Chang, J. (2021). MorphEst: An automated toolbox for measuring estuarine planform geometry from remotely sensed imagery and its application to the South Korean Coast [Software]. Remote Sensing, *13*(2), 330. https://doi.org/10.3390/rs13020330

Kennish, M. J. (2002). Environmental threats and environmental future of estuaries. *Environmental Conservation*, *29*(1), 78–107. https://doi.org/10.1017/s0376892902000061

Kim, T. I., Choi, B. H., & Lee, S. W. (2006). Hydrodynamics and sedimentation induced by large-scale coastal developments in the Keum River Estuary, Korea. *Estuarine, Coastal and Shelf Science*, *68*(3–4), 515–528. https://doi.org/10.1016/j.ecss.2006.03.003

Kirwan, M. L., & Megonigal, J. P. (2013). Tidal wetland stability in the face of human impacts and sea-level rise. *Nature*, *504*(7478), 53–60. https://doi.org/10.1038/nature12856

Koehnken, L., Rintoul, M. S., Goichot, M., Tickner, D., Loftus, A.-C., & Acreman, M. C. (2020). Impacts of riverine sand mining on freshwater ecosystems: A review of the scientific evidence and guidance for future research. *River Research and Applications*, *36*(3), 362–370. https://doi.org/10.1002/rra.3586

Latrubesse, E. M., Arima, E. Y., Dunne, T., Park, E., Baker, V. R., d'Horta, F. M., et al. (2017). Damming the rivers of the Amazon basin. *Nature*, *546*(7658), 363–369. https://doi.org/10.1038/nature22333

Maddison, A. (2010). Historical statistics of the world economy: 1-2008 AD [Dataset]. Retrieved from https://www.rug.nl/ggdc/historicaldevelopment/maddison/releases/maddison-database-2010

Nicholls, R. J., Adger, W. N., Hutton, C. W., & Hanson, S. E. (2020). *Deltas in the Anthropocene*. Springer Nature. https://doi.org/10.1007/978-3-030-23517-8

Nienhuis, J. H., Ashton, A. D., Edmonds, D. A., Hoitink, A. J. F., Kettner, A. J., Rowland, J. C., & Törnqvist, T. E. (2020). Global-scale human impact on delta morphology has led to net land area gain. *Nature*, *577*(7791), 514–518. https://doi.org/10.1038/s41586-019-1905-9

Pekel, J.-F., Cottam, A., Gorelick, N., & Belward, A. S. (2016). High-resolution mapping of global surface water and its long-term changes [Dataset]. Nature, *540*(7633), 418–422. https://doi.org/10.1038/nature20584

Powell, R. D., & Molnia, B. F. (1989). Glacimarine sedimentary processes, facies and morphology of the south-southeast Alaska shelf and fjords. *Marine Geology*, *85*(2–4), 359–390. https://doi.org/10.1016/0025-3227(89)90160-6

Prandle, D. (2004). How tides and river flows determine estuarine bathymetries. *Progress in Oceanography*, *61*, 1–26. https://doi.org/10.1016/j.pocean.2004.03.001

Raabe, E. A., & Stumpf, R. P. (2016). Expansion of tidal marsh in response to sea-level rise: Gulf Coast of Florida, USA. *Estuaries and Coasts*, *39*(1), 145–157. https://doi.org/10.1007/s12237-015-9974-y

Renaud, F. G., Syvitski, J. P. M., Sebesvari, Z., Werners, S. E., Kremer, H., Kuenzer, C., et al. (2013). Tipping from the Holocene to the Anthropocene: How threatened are major world deltas? *Current Opinion in Environmental Sustainability*, *5*(6), 644–654. https://doi.org/10.1016/j.cosust.2013.11.007

Rodriguez, A. B., McKee, B. A., Miller, C. B., Bost, M. C., & Atencio, A. N. (2020). Coastal sedimentation across North America doubled in the 20th century despite river dams. *Nature Communications*, *11*(1), 3249. https://doi.org/10.1038/s41467-020-16994-z

Savenije, H. H. G. (2005). *Salinity and tides in alluvial estuaries*. Gulf Professional Publishing.

Scharfe, W. (2018). *Abriss der Kartographie Brandenburgs 1771–1821*. Walter de Gruyter GmbH & Co KG.

Schieder, N. W., & Kirwan, M. L. (2019). Sea-level driven acceleration in coastal forest retreat. *Geology*, *47*(12), 1151–1155. https://doi.org/10.1130/g46607.1

Schieder, N. W., Walters, D. C., & Kirwan, M. L. (2018). Massive upland to wetland conversion compensated for historical Marsh Loss in Chesapeake Bay, USA. *Estuaries and Coasts*, *41*(4), 940–951. https://doi.org/10.1007/s12237-017-0336-9

Sengupta, D., Choi, Y. R., Tian, B., Brown, S., Meadows, M., Hackney, C. R., et al. (2023). Mapping 21st century global coastal land reclamation. *Earth's Future*, *11*(2), e2022EF002927. https://doi.org/10.1029/2022ef002927

Shin, H.-J., Lee, G., Kang, K., & Park, K. (2019). Shift of estuarine type in altered estuaries. *Anthropocene Coasts*, *2*(1), 145–170. https://doi.org/10.1139/anc-2018-0013

Smits, A. J. M., Nienhuis, P. H., & Saeijs, H. L. F. (2006). Changing estuaries, changing views. *Hydrobiologia*, *565*(1), 339–355. https://doi.org/10.1007/s10750-005-1924-4

Syvitski, J. P. M., Angel, J. R., Saito, Y., Overeem, I., Vörösmarty, C., Wang, H., & Olago, D. (2022a). Earth's sediment cycle during the Anthropocene. *Nature Reviews Earth & Environment*, *3*, 179–196. https://doi.org/10.1038/s43017-021-00253-w

Syvitski, J. P. M., Anthony, E., Saito, Y., Zainescu, F., Day, J., Bhattachary, J. P., & Giosan, L. (2022b). Large deltas, small deltas: Toward a more rigorous understanding of coastal marine deltas. *Global and Planetary Change*, *218*, 103958. https://doi.org/10.1016/j.gloplacha.2022.103958

Syvitski, J. P. M., & Kettner, A. J. (2011). Sediment flux and the Anthropocene. *Philosophical Transactions of the Royal Society A*, *369*(1938), 957–975. https://doi.org/10.1098/rsta.2010.0329

Syvitski, J. P. M., Kettner, A. J., Overeem, I., Hutton, E. W. H., Hannon, M. T., Brakenridge, G. R., et al. (2009). Sinking deltas due to human activities. *Nature Geoscience*, *2*(10), 681–686. https://doi.org/10.1038/ngeo629

Syvitski, J. P. M., & Saito, Y. (2007). Morphodynamics of deltas under the influence of humans. *Global and Planetary Change*, *57*(3–4), 261–282. https://doi.org/10.1016/j.gloplacha.2006.12.001

Syvitski, J. P. M., Vörösmarty, C. J., Kettner, A. J., & Green, P. (2005). Impact of humans on the flux of terrestrial sediment to the global coastal ocean. *Science*, *308*(5720), 376–380. https://doi.org/10.1126/science.1109454

Tessler, Z. D., Vörösmarty, C. J., Grossberg, M., Gladkova, I., Aizenman, H., Syvitski, J. P., & Foufoula-Georgiou, E. (2015). Profiling risk and sustainability in coastal deltas of the world. *Science*, *349*(6248), 638–643. https://doi.org/10.1126/science.aab3574
Traini, C., Proust, J.-N., Menier, D., & Mathew, M. J. (2015). Distinguishing natural evolution and human impact on estuarine morpho-sedimentary development: A case study from the Vilaine Estuary, France. *Estuarine, Coastal and Shelf Science*, *163*, 143–155. https://doi.org/10.1016/j.ecss.2015.06.025
van der Wal, D., Pye, K., & Neal, A. (2002). Long-term morphological change in the Ribble Estuary, northwest England. *Marine Geology*, *189*(3–4), 249–266. https://doi.org/10.1016/s0025-3227(02)00476-0
van Maren, D. S., Oost, A. P., Wang, Z. B., & Vos, P. C. (2016). The effect of land reclamations and sediment extraction on the suspended sediment concentration in the Ems Estuary. *Marine Geology*, *376*, 147–157. https://doi.org/10.1016/j.margeo.2016.03.007
Wang, W., Liu, H., Li, Y., & Su, J. (2014). Development and management of land reclamation in China. *Ocean & Coastal Management*, *102*, 415–425. https://doi.org/10.1016/j.ocecoaman.2014.03.009
Wei, X., Cai, S., & Zhan, W. (2021). Impact of anthropogenic activities on morphological and deposition flux changes in the Pearl River Estuary, China. *Scientific Reports*, *11*(1), 16643. https://doi.org/10.1038/s41598-021-96183-0
Wei, X., Cai, S., Zhan, W., & Li, Y. (2021). Changes in the distribution of surface sediment in Pearl River Estuary, 1975-2017, largely due to human activity. *Continental Shelf Research*, *228*, 104538. https://doi.org/10.1016/j.csr.2021.104538
Williams, J. R., Dellapenna, T., Lee, G., & Louchouarn, P. (2014). Sedimentary impacts of anthropogenic alterations on the Yeongsan Estuary, South Korea. *Marine Geology*, *357*, 256–271. https://doi.org/10.1016/j.margeo.2014.08.004
Williams, J. R., Dellapenna, T. M., & Lee, G. (2013). Shifts in depositional environments as a natural response to anthropogenic alterations: Nakdong Estuary, South Korea. *Marine Geology*, *343*, 47–61. https://doi.org/10.1016/j.margeo.2013.05.010
Williams, J. R., Lee, G., Shin, H.-J., & Dellapenna, T. (2015). Mechanism for sediment convergence in the anthropogenically altered microtidal Nakdong Estuary, South Korea. *Marine Geology*, *369*, 79–90. https://doi.org/10.1016/j.margeo.2015.08.004
Wolanski, E., Moore, K., Spagnol, S., D'Adamo, N., & Pattiaratchi, C. (2001). Rapid, human-induced siltation of the macro-tidal Ord River Estuary, Western Australia. *Estuarine, Coastal and Shelf Science*, *53*(5), 717–732. https://doi.org/10.1006/ecss.2001.0799
Wulf, M., & Rujner, H. (2011). A GIS-based method for the reconstruction of the late eighteenth century forest vegetation in the Prignitz region (NE Germany). *Landscape Ecology*, *26*(2), 153–168. https://doi.org/10.1007/s10980-010-9555-1
Young, S. M., & Ishiga, H. (2014). Assessment of dam removal from geochemical examination of Kuma River sediment, Kyushu, Japan. *Environmental Monitoring and Assessment*, *186*(12), 8267–8289. https://doi.org/10.1007/s10661-014-4002-4
Ysebaert, T., van der Hoek, D.-J., Wortelboer, R., Wijsman, J. W. M., Tangelder, M., & Nolte, A. (2016). Management options for restoring estuarine dynamics and implications for ecosystems: A quantitative approach for the Southwest Delta in the Netherlands. *Ocean & Coastal Management*, *121*, 33–48. https://doi.org/10.1016/j.ocecoaman.2015.11.005

References From the Supporting Information

Caldwell, R. L., Edmonds, D. A., Baumgardner, S., Paola, C., Roy, S., & Nienhuis, J. H. (2019). A global delta dataset and the environmental variables that predict delta formation on marine coastlines. *Earth Surface Dynamics*, *7*(3), 773–787. https://doi.org/10.5194/esurf-7-773-2019
Edmonds, D. A., Caldwell, R. L., Brondizio, E. S., & Siana, S. M. O. (2020). Coastal flooding will disproportionately impact people on river deltas. *Nature Communications*, *11*(1), 4741. https://doi.org/10.1038/s41467-020-18531-4
Reeve, D. E., & Karunarathna, H. (2009). On the prediction of long-term morphodynamic response of estuarine systems to sea level rise and human interference. *Continental Shelf Research*, *29*(7), 938–950. https://doi.org/10.1016/j.csr.2009.01.010